Minimax Theory and its Applications
Volume 11 (2026), No. 2s, 447-460

A minimax robust learning framework for uncertainty-aware indoor localization in LoRaWAN networks using adaptive signal filtering and environmental intelligence

S. Daphine Sherin Mancy[1], Dr.D. David Neels Ponkumar[2], Dr.G. Aravind Swaminathan[3], Dr.K. Balamurugan[4]

[1]Research Scholar, Department of Electronics and Communication Engineering, VelTech Rangarajan Dr. Sagunthala R&D Institute of Science and Technology, Chennai, Tamil Nadu, India. mancysherin@gmail.com

[2]Professor, Department of ECE, Vel Tech Rangarajan Dr. Sagunthala R&D Institute of Science and Technology, Chennai, Tamil Nadu, India. david26571@gmail.com

[3]Professor, Department of Computer Science and Engineering, Francis Xavier Engineering College, Tirunelveli, Tamil Nadu, India. aravindswaminathan.g@francisxavier.ac.in, https://orcid.org/0009-0009-0733-4656

[4]Professor, Department of Electronics and Communication Engineering, Saveetha School of Engineering, Saveetha Institute of Medical and Technical Sciences, (SIMATS), Chennai, India. bala237115@gmail.com, balamurugank.sse@saveetha.com

Abstract

LoRaWAN is increasingly used for indoor Internet-of-Things sensing, but its received signal strength indicator (RSSI) is heavily perturbed by multipath, human blockage, wall structure, and microclimate dynamics, so ranging methods built only to minimize average error give no guarantee about the worst case. This paper treats indoor LoRaWAN ranging as a minimax robust estimation problem. We couple an environment-aware multi-wall path-loss model with a Minimax Robust Adaptive Filter (MRAF), which applies a Huber-type bounded-influence correction to the RSSI innovation together with an environmentally driven process-noise schedule, and we prove that the resulting one-step innovation risk stays bounded over an epsilon-contamination neighborhood of the nominal noise model, unlike the corresponding unbounded Kalman correction. The framework is tested on 1,715,869 aggregated uplinks collected over roughly eight months from six statically deployed end devices, 8 to 40 meters from a single gateway, with 0 to 2 concrete walls and 0 to 5 wooden walls per link. Against raw RSSI, a moving-average filter, and a standard Kalman filter, the proposed method reduces mean ranging RMSE from 92.0 m to 8.4 m and reduces the worst-case RMSE across the six links from 160.9 m to 11.7 m, degrading by only 15.8% under adverse channel conditions versus 31.5% for the standard Kalman filter. These results indicate that explicit minimax-robust, environment-aware filtering is a theoretically grounded and practically inexpensive route to uncertainty-aware indoor localization.

Keywords: Minimax estimation, robust filtering, indoor localization, LoRaWAN, adaptive filtering, uncertainty quantification.

2020 Mathematics Subject Classification: *90C47 (Minimax problems); 62C20 (Minimax estimation); 93E11 (Filtering in stochastic control); 68T05 (Learning and adaptive systems).*

1. Introduction

Getting a device's location right indoors turns out to be a much harder problem than doing the same thing

outdoors. The main reason is that satellite navigation, the one technology built specifically for the job, simply does not reach through walls and floors in any useful way. Low-power wide-area network (LPWAN) technologies have become a popular workaround for indoor Internet-of-Things (IoT) deployments because they sidestep this problem differently (Soma, 2025). A single LoRaWAN gateway can serve hundreds of low-cost, battery-powered end devices across ranges of tens of meters indoors, and the same uplink traffic that already carries sensor data can, in principle, be repurposed for ranging (Obiri & Van Laerhoven, 2024, 2026). However, it must be noted that the RSSI, which is the only distance-related variable that can be determined using no additional hardware, is influenced by a number of factors: the distance-dependent attenuation (path loss), the attenuation caused by walls and floors, multipath fading, human activity in the environment, and the long-term drift that depends on the heating and cooling cycles. This makes it quite reasonable for the RSSI-based ranging to end up within the 8 to 20 m accuracy range (Rathnayake et al., 2023; Vo et al., 2024; Obiri & Van Laerhoven, 2026a).

Two different approaches have been proposed to handle this. The first one takes advantage of physics. It uses an inverse path loss model, like the COST-231 multi-wall model, to calculate a distance from an observed path loss (European Commission, 1999). Physics-based models are inexpensive and intuitive, but they are created under the assumption of a static environment, which does not persist for very long. In particular, changes in temperature and humidity are known to cause errors in distance estimation when the environment becomes different from what it used to be at the time the model was fitted (Azevedo & Mendonça, 2024; Lavdas et al., 2021; Obiri & Van Laerhoven, 2026a). The second approach is more data-driven and uses either fingerprinting, or random forests, or deep networks trained on examples to learn the complex relations between RSSI, SNR, and the environmental context. They may prove to be reasonably accurate at the particular location they have been trained in, but in general, they require labeled data for calibration and do not perform well once the conditions move away from the training distribution. What is more important is the fact that they make no mention whatsoever regarding the worst-case scenario, which is precisely where such systems eventually end up.

The authors of the paper believe that ranging in indoor LoRaWAN environment should be seen as a problem of minimax robust estimation from the very beginning, and not as an average-error minimization problem (Basar & Bernhard, 1995; Obiri & Van Laerhoven, 2025a). Concretely, we design a filter meant to bound the worst-case estimation risk over a family of plausible contaminating noise distributions, of the kind produced by multipath bursts, blockage events, and sudden environmental changes, while an environment-aware multi-wall path-loss model supplies the physical mapping from signal to distance. The aim is to keep the interpretability and low cost that make physics-based ranging attractive, while adding a robustness property that purely average-case adaptive filters simply do not provide.

This paper makes four contributions.

- It formulates uncertainty-aware indoor LoRaWAN ranging as a minimax robust estimation problem, and derives a Minimax Robust Adaptive Filter (MRAF) that pairs a Huber-type bounded-influence correction of RSSI innovations with an environmentally driven process-noise schedule, together with a worst-case error bound grounded in Huber's minimax estimation theory (Ferrari et al., 2025).
- It fits and validates an environment-aware multi-wall path-loss model on a large, eight-month indoor LoRaWAN dataset covering six links with markedly different distances (8-40 m) and wall compositions, and the resulting wall-attenuation coefficients line up closely with values reported independently for a comparable deployment (Obiri & Van Laerhoven, 2025a).
- This study uses a robust metric of range estimation accuracy and an analysis of unfavorable versus favorable conditions for link communication, rather than mean-error metrics only, proving that the proposed filter reduces both the mean and dispersion of the risk associated with a heterogeneous collection of links.
- The proposed approach is compared to the raw RSSI measure, moving average filtering, conventional Kalman filter, and recent research on environment-aware LoRaWAN ranging, all using the same testbed.

The remainder of the paper proceeds as follows. In Section 2, we provide a review of relevant literature pertaining to LoRaWAN ranging indoors, propagation effects, and minimax or robust filtering theory. In Section 3, the dataset and its testbed are described. In Section 4, we provide the proposed framework that includes a path-loss model, an adaptive filter, and an analytically robustness result. Section 5 deals with the experimental setup, while the results are presented in Section 6. The limitations are discussed in Section 7, and Section 8 contains conclusions and future directions.

2. Related work

2.1 RSSI- and path-loss-based LoRaWAN indoor ranging

RSSI has stayed the go-to observable for LoRaWAN ranging simply because it costs nothing extra: it is already

sitting in every received packet. The classical route inverts a log-distance or multi-wall path-loss law (European Commission, 1999). Vo et al., (2024) extend the plain log-distance model with additional correction terms and report meaningful accuracy gains over the unmodified baseline. González-Palacio et al., (2023) blend machine learning with a physical path-loss-and-shadowing model to improve both accuracy and energy efficiency in LoRaWAN networks. Wang et al., (2025) build a weighted hybrid positioning method around explicit path-loss-exponent estimation, a useful reminder that exponent-aware ranging has not been made obsolete by data-driven methods (Wang et al., 2025). The work closest to what is presented here is a series of studies by Obiri and Van Laerhoven, who instrumented a one-year, six-device, single-gateway indoor LoRaWAN testbed and developed an environment-aware multi-wall path-loss model (MWM-EP) paired with an innovation-driven, self-tuning Kalman prefilter (MWM-EP-KF) (Khodarahmi & Maihami, 2023). Their pipeline reaches 4.74 m mean absolute error (MAE) and 6.76 m RMSE under an 80/20 chronological train-test split with device-wise anomaly removal (Obiri & Van Laerhoven, 2026b). Companion papers characterize the same testbed through regression and ANOVA (Obiri & Van Laerhoven, 2025b), shadow-fading calibration (Obiri & Van Laerhoven, 2026a), and a full description of the measurement campaign itself (Obiri & Van Laerhoven, 2025a). The measurements analyzed in the present study come from the same class of testbed, namely six static end devices at 8 to 40 m from a single gateway, with recorded concrete and wooden wall counts and co-located environmental sensing, so Section 6.5 uses the reported MWM-EP-KF figures as a direct point of comparison. Recent survey work confirms that RSSI- and fingerprinting-based indoor localization, LoRa included, remains an active area where robustness and generalization are still open problems (Ahmad, 2024; Aziz & Koo, 2025; Rathnayake et al., 2023).

2.2 Environmental effects on indoor RF propagation

Temperature and humidity do more than provide context to 868 MHz propagation; they affect it physically by causing absorption via water vapor and changes in the dielectric properties of building materials. This effect is quantified in the case of an indoor LoRa propagation model by Lavdas et al., (2021), who find measurable changes in the path loss parameters estimated from such a model under different seasonal conditions. The work of Azevedo & Mendonça, (2024), who survey propagation models that have been used in LoRa networks, highlights how structural models tuned under one set of environmental conditions quickly become inaccurate as these conditions deviate from the norm – precisely the thing one would expect once the underlying physics becomes clear. Occupancy by humans provides a second, fast-changing source of propagation attenuation and scattering on top of that. The combination of these observations makes it clear why environmental covariates are treated as model inputs here, on par with the approach in Obiri and Van Laerhoven, (2025a, 2026a).

2.3 Robust and minimax filtering theory

Under exactly known Gaussian noise, the Kalman filter is the optimal linear estimator, full stop. The trouble starts when that noise model is wrong, which it usually is to some degree in an indoor RSSI stream disturbed by transient blockage and multipath bursts (Hasan et al., 2025). Under exactly that kind of contamination, the filter's performance can fall apart quickly. Robust statistics gets around this by swapping the quadratic loss for a bounded-influence loss. Huber, (1992) showed that, for an epsilon-contamination neighborhood around a nominal Gaussian distribution, there is an estimator that minimizes the maximum asymptotic variance over that whole neighborhood, which is a minimax robust estimator in the strict sense (Wald, 1950). The same idea carries over into dynamic state estimation through H-infinity and game-theoretic minimax filtering, which minimizes worst-case error over bounded-energy disturbances instead of expected error under a single fixed noise model (Anwar & Zhu, 2017; Mitter, 1996). Related self-tuning and maximum-correntropy variants have already found their way into wireless sensor network positioning (Liao et al., 2022). Underneath both Huber's estimator and H-infinity filtering sits the older statistical-decision-theoretic notion of a minimax rule, which says to pick the rule that minimizes the maximum risk over an uncertain state of nature (Wald, 1950). Even with this theoretical background available, existing LoRaWAN ranging pipelines, including the innovation-driven adaptive Kalman filter used in Obiri and Van Laerhoven, (2026b), adapt the measurement-noise covariance online but stop short of a bounded-influence, minimax-robust correction of the innovation itself, and none of them report worst-case-over-link risk explicitly. That is the gap this paper tries to close, by combining a Huber-type minimax-robust innovation correction with an environment-driven adaptive process-noise schedule, and by reporting minimax metrics alongside the usual average-case numbers.

3. Materials: dataset and experimental testbed

The dataset behind this study is a set of 1,715,869 aggregated uplink records, collected between 26 September 2024 and 22 May 2025. That span covers roughly eight months, long enough to catch a couple of seasonal transitions, from six statically deployed LoRaWAN end devices (labeled ED0 through ED5) reporting to one indoor gateway at a nominal 60-second interval. This matches the testbed and reporting cadence described for the same class of deployment in Obiri & Van Laerhoven, (2025a, 2026b). Each uplink record combines LoRaWAN radio-link metrics with co-located environmental readings across twenty fields: a UTC timestamp, a

device identifier, CO2 concentration (ppm), relative humidity (%), fine particulate matter (PM2.5, µg/m³), barometric pressure (hPa), temperature (°C), RSSI (dBm), SNR (dB), spreading factor, carrier frequency, frame and packet sequence counters, a time-on-air proxy, the ground-truth transmitter-receiver distance (m), counts of intervening concrete/brick and wooden walls, and three pre-computed propagation quantities (expected path loss, estimated noise power, and estimated signal power) retained in the aggregation mainly for cross-checking. Table 1 lays out the per-device geometry alongside the mean RSSI recorded at SF7, which we use later as the least airtime-distorted reference point for calibrating the path-loss model in Section 4.2.

Table 1: Per-link deployment geometry and reference (SF7) mean RSSI.

Device	Distance (m)	Concrete walls	Wooden walls	Mean RSSI @ SF7 (dBm)	Records
ED0	10	0	0	-49.29	285,563
ED1	8	1	0	-56.46	283,911
ED2	23	0	2	-69.96	287,019
ED3	18	1	2	-70.84	283,068
ED4	37	0	5	-83.20	281,880
ED5	40	2	2	-96.38	294,428

The dataset spans spreading factors SF7 through SF12 (318,321; 316,520; 304,377; 291,178; 239,878; and 245,595 packets, respectively), which gives a fairly wide spread of link margins and airtimes within a single deployment. Accordingly, RSSI noise is highly diverse as well because the adaptive data rate feature in LoRaWAN technology increases the spreading factor as the link gets worse. The range of RSSI values spans from -128 dBm to -28 dBm (mean: -76.7 dBm, SD: 22.6 dB) and is caused by a combination of all the four factors discussed above – namely distance, attenuation, sensitivity depending on the spreading factor, and fading. These four factors are the exact combination necessary for the testing of the filter's performance at its worst case in an operational envelope, which is the primary objective of minimax robust design.

4. Proposed minimax robust learning framework

4.1 Problem formulation and notation

Consider a fixed link ℓ (an end device paired with the gateway) at a known, static separation d_ℓ. Let $z_{\ell,k}$ be the RSSI reported in the k-th received packet, and let e_k collect the environmental covariates (temperature, relative humidity, barometric pressure) recorded at that same time. The overall pipeline has two stages: a static, environment-aware path-loss model that turns a (possibly filtered) RSSI value plus the link's wall counts into a distance estimate, and a causal, per-link filter $\hat{x}_k$ that turns the raw stream $\{z_{\ell,1},\ldots,z_{\ell,k}\}$ into a refined RSSI estimate. What we want from the filter is not the smallest expected squared ranging error on its own, but the smallest worst-case ranging risk over a set $\mathcal{P}_\varepsilon$ of plausible innovation-noise distributions, of the kind produced by multipath bursts, blockage, and fast environmental swings. That amounts to approximately solving

$$\min_f \quad \max_{P \in \mathcal{P}_\varepsilon} \quad E_P[(\hat{d}_k - d_\ell)^2],$$

and this is the working definition of minimax robustness used throughout the rest of the paper.

4.2 Environment-aware multi-wall path-loss model

Distance inversion uses a log-distance multi-wall path-loss model in the spirit of the COST-231 MWM and its environment-augmented descendants (European Commission, 1999; Obiri & Van Laerhoven, 2026b):

$$L(d) = \beta_0 + 10\, n\, log_{10}(d / d_0) + \kappa_c\, C_{walls} + \kappa_w\, W_{walls} + \psi,$$

Where L(d) = -RSSI is the observed path loss, β_0 is a site-calibrated intercept, n is the path-loss exponent, d_0 = 1 m is the reference distance, C_{walls} and W_{walls} are the concrete/brick and wooden wall counts on that link, κ_c and κ_w are the corresponding per-wall attenuation coefficients, and ψ absorbs whatever shadowing is left over. The four structural parameters (β_0, n, κ_c, κ_w) were fit by ordinary least squares on the six device-level reference points in table 1, restricted to SF7 packets to keep spreading-factor noise out of the calibration. Section 6.1 reports and discusses the fitted values; at inference time the model is inverted deterministically to map a raw or filtered RSSI reading onto a distance estimate,

$$\hat{d} = d_0 \cdot 10^{\frac{-RSSI - \beta_0 - \kappa_c\, C_{walls} - \kappa_w\, W_{walls}}{10\, n}}.$$

With only six links available for structural calibration, this part of the framework is deliberately kept small and interpretable. The environmental sensitivity of ranging is instead handled dynamically, inside the filter, which is

where we turn next.

4.3 Minimax robust adaptive filter (MRAF)

The proposed filter processes each link's RSSI stream independently through a scalar, forward-only recursion built from two pieces working together: a bounded-influence, Huber-type correction of the innovation, which is where the minimax robustness against an epsilon-contamination neighborhood of the nominal innovation distribution comes from (Huber, 1992), and an environment-driven process-noise term that opens the filter's trust region wider during rapid environmental change and pulls it back in otherwise. At each step k, given the previous estimate $\hat{x}_{k-1}$ and its covariance P_{k-1}, the filter first computes an environment-driven process noise,

$$Q_k = Q_0 \cdot (1 + 3\, v_k), \quad v_k = clip\left(\frac{\|\Delta e_k\|}{\sigma_{\Delta e}}, 0, 5\right),$$

Where v_k is a normalized volatility signal built from the per-step rate of change of temperature, relative humidity, and pressure, and $\sigma_{\Delta e}$ is a per-covariate scale estimated from the training stream. The predicted state and covariance follow a random-walk model, $\hat{x}_{k|k-1} = \hat{x}_{k-1}$ and $P_{k|k-1} = P_{k-1} + Q_k$, which is reasonable given how slowly path loss actually moves over a 60-second reporting window. The innovation $\nu_k = z_k - \hat{x}_{k|k-1}$ is standardized as $s_k = \nu_k / \hat{\sigma}$ using a robust, median-absolute-deviation-based scale estimate of the innovation stream, and then passed through Huber's bounded-influence function,

$$\psi_c(s_k) = s_k \;\; if\; |s_k| \le c, \quad \psi_c(s_k) = c \cdot sign(s_k) \;\; if\; |s_k| > c,$$

With threshold c = 1.345, the standard choice, giving 95% efficiency relative to the sample mean under the nominal Gaussian model while still bounding how much influence any single innovation can have (Huber, 1964). Flagged outliers inflate the measurement-noise term, $R_k = R_0 \cdot (1 + 0.5 \cdot 1\{|s_k| > c\})$, and the filter then runs the ordinary Kalman gain and update, $K_k = P_{k|k-1} / (P_{k|k-1} + R_k)$, $\hat{x}_k = \hat{x}_{k|k-1} + K_k \cdot \hat{\sigma} \cdot \psi_c(s_k)$, and $P_k = (1 - K_k) \cdot P_{k|k-1}$, using the bounded-influence-corrected innovation rather than the raw one. The net effect is a filter that behaves much like an ordinary, environment-adaptive Kalman filter when conditions are nominal, but that automatically caps the damage any single anomalous packet can do, so that neither an isolated deep fade nor a sudden environmental spike can send the distance estimate flying off unbounded.

4.4 Preliminary definitions

Definition 1 (Epsilon-contamination neighborhood). Let $F_0 = N(0, \sigma^2)$ be a nominal Gaussian innovation law, and let $\varepsilon \in [0, 1)$ be a contamination fraction. The epsilon-contamination neighborhood of F_0 is

$$\mathcal{P}_\varepsilon(F_0) = \{\, (1 - \varepsilon) F_0 + \varepsilon\, H \;:\; H \; is \; an \; arbitrary \; probability \; distribution \; on \; \mathbb{R} \,\}.$$

A distribution in $\mathcal{P}_\varepsilon(F_0)$ corresponds to a nominal Gaussian innovation process, which is contaminated with probability ε, to take on any arbitrary contaminating value; this is the classical model for multipath bursts, blockages, or faulty sensors that override the RSSI signal at times.

Definition 2 (Minimax robust score). For translation-invariant M-estimators with score functions ψ, which are odd, nondecreasing, and bounded, a ψ, a score ψ* is minimax robust over $\mathcal{P}_\varepsilon(F_0)$ if

$$\psi* \in \; argmin_\psi \;\; sup_{P \in \mathcal{P}_\varepsilon(F_0)} \;\; V(\psi, P),$$

Where V(ψ, P) denotes the asymptotic variance of the M-estimator induced by ψ under P. This is the classical minimax approach adapted to selecting the score function directly.

Lemma 1 (Boundedness and Lipschitz continuity of the Huber score). The Huber score.

$$\psi_c(s) \;=\; max\big(-c, min(s,c)\big), \quad s \;\in\; \mathbb{R}, c \;>\; 0,$$

Satisfies (i) $|\psi_c(s)| \le c$ for every $s \in \mathbb{R}$; (ii) ψ_c is odd, nondecreasing, and 1-Lipschitz, i.e., $|\psi_c(s1) - \psi_c(s2)| \le |s1 - s2|$ for all $s1, s2 \in \mathbb{R}$; and (iii) $\psi_c(s) = s$ whenever $|s| \le c$.

Proof. Property (iii) and oddness follow immediately from the definition. For (i), if $|s| \le c$ then $\psi_c(s) = s$ and $|\psi_c(s)| = |s| \le c$; if $s > c$ then $\psi_c(s) = c$; if $s < -c$ then $\psi_c(s) = -c$. In every case $|\psi_c(s)| \le c$. For (ii), monotonicity holds because ψ_c is the composition of the identity with clipping to $[-c, c]$, which is monotone, and the Lipschitz bound follows because the derivative of ψ_c is 1 on $(-c, c)$ and 0 elsewhere, so $|\psi_c(s1) - \psi_c(s2)| \le |s1 - s2|$ by the mean value theorem applied piecewise.

4.5 Main robustness theorem

Theorem 1 (Minimax property of the Huber correction and bounded worst-case innovation risk). Let $F_0 = N(0, \sigma^2)$ and let $\mathcal{P}_\varepsilon(F_0)$ be as in Definition 1, for $\varepsilon \in [0, 0.5)$. Then:

(a) [Huber, 1964] There exists a threshold $c = c(\varepsilon, \sigma) > 0$, the unique solution of

$$2\varphi(c) \,/\, c \;-\; 2\Phi(-c) \;=\; \frac{\varepsilon}{1 \;-\; \varepsilon},$$

Where φ and Φ are the standard normal density and distribution function, such that ψ_c is minimax robust over $\mathcal{P}_\varepsilon(F_0)$ in the sense of Definition 2; the corresponding least-favorable distribution has a density proportional to φ on $[-c, c]$ and to exponential tails outside that interval.

(b) For this or any fixed $c > 0$, the one-step contribution of the innovation to the MRAF state update, $K_k \cdot \hat{\sigma} \cdot \psi_c(s_k)$, satisfies

$$sup_{P \,\in\, \mathcal{P}_\varepsilon(F_0)} \; E_P\left[\left(K_k \;\hat{\sigma}\; \psi_c(s_k)\right)^2\right] \;\le\; (K_k \;\hat{\sigma}\; c)^2 \;<\; \infty,$$

Uniformly over $\varepsilon \in [0, 1)$, whereas the corresponding uncorrected (ordinary Kalman) innovation term $K_k \cdot \nu_k$ satisfies

$$sup_{P \,\in\, \mathcal{P}_\varepsilon(F_0)} \; E_P[(K_k \;\nu_k)^2] \;=\; +\infty \quad for\; every\; \varepsilon \;>\; 0.$$

Proof. Part (a) is Huber's classical result (Huber, 1992); it is restated here because it identifies the specific ψ_c used in Section 4.3 as the minimax-optimal choice for this problem, rather than an arbitrary bounded-influence heuristic, and we omit the full derivation of the least-favorable density, referring the reader to the original source.

For part (b), fix any $P \in \mathcal{P}_\varepsilon(F_0)$ and let $\nu \sim P$. By Lemma 1(i), $|\psi_c(s)| \le c$ almost surely for every realization of the standardized innovation $s = \nu/\hat{\sigma}$, so $|K_k \;\hat{\sigma}\; \psi_c(s)| \le K_k \;\hat{\sigma}\; c$ pointwise, and therefore $(K_k \;\hat{\sigma}\; \psi_c(s))^2 \le (K_k \;\hat{\sigma}\; c)^2$ almost surely. Taking expectations under P preserves this pointwise bound, so $E_P[(K_k \;\hat{\sigma}\; \psi_c(s))^2] \le (K_k \;\hat{\sigma}\; c)^2$ for every $P \in \mathcal{P}_\varepsilon(F_0)$, including the least-favorable one; taking the supremum over $\mathcal{P}_\varepsilon(F_0)$ therefore gives $sup_P \; E_P[(K_k \;\hat{\sigma}\; \psi_c(s))^2] \le (K_k \;\hat{\sigma}\; c)^2$, which is finite and does not depend on ε. This proves the first claim.

For the second claim, fix $\varepsilon > 0$ and, for $n = 1, 2, 3, \ldots$, let H_n be the point mass at $\nu = n\hat{\sigma}$. Then $P_n = (1-\varepsilon)F_0 + \varepsilon H_n \in \mathcal{P}_\varepsilon(F_0)$, and $E_{P_n}[(K_k \;\nu)^2] \ge \varepsilon \cdot (K_k \cdot n\hat{\sigma})^2$, which diverges to $+\infty$ as $n \to \infty$. Since $\{P_n\} \subset \mathcal{P}_\varepsilon(F_0)$, the supremum over the whole neighborhood is unbounded, so $sup_P \; E_P[(K_k \;\nu)^2] = +\infty$.

Theorem 1 formalizes, for the innovation-correction step of the MRAF recursion, the informal robustness claim motivating the design in Section 4.3: the Huber-corrected update carries a worst-case one-step risk that is bounded uniformly over the entire contamination class, while the ordinary Kalman update does not. This is the mathematical content behind the empirical worst-case comparisons of Section 6.3, where the MRAF compresses the maximum-over-link RMSE relative to the non-robust baseline.

4.6 Boundedness of the filter covariance

A second, complementary stability property concerns the error covariance sequence $\{P_k\}$ itself, independent of any distributional assumption on the innovations.

Lemma 2 (Uniform boundedness of the estimation covariance). Suppose the process noise Q_k and measurement noise R_k in the MRAF recursion of Section 4.3 satisfy $Q_k \in [Q_{min}, Q_{max}]$ and $R_k \in [R_{min}, R_{max}]$ for all k, with $Q_{min}, R_{min} > 0$, as guaranteed by the clipped volatility signal $v_k \in [0, 5]$ and the bounded outlier-inflation factor in R_k. Then, for every k ≥ 1,

$$0 \;<\; P_k \;\leq\; R_{max}.$$

Proof. Write $S_{k|k-1} = P_{k-1} + Q_k > 0$ for the predicted variance. The Kalman gain is $K_k = S_{k|k-1} / (S_{k|k-1} + R_k)$, and the updated covariance is

$$P_k \;=\; (1 \;-\; K_k) \;\cdot\; S_{k|k-1} \;=\; \frac{S_{k|k-1} \;\cdot\; R_k}{S_{k|k-1} \;+\; R_k}.$$

Since $S_{k|k-1} > 0$ and $R_k > 0$, the factor $S_{k|k-1} / (S_{k|k-1} + R_k)$ lies strictly in (0, 1), so $P_k < R_k \leq R_{max}$. Positivity, $P_k > 0$, follows because P_k is a ratio of strictly positive quantities. And it is true for each k, including k = 1 (since $P_0 > 0$ by initialization), Thus, the bound is established for all k ≥ 1 by direct substitution rather than induction.

Lemma 2 guarantees that the MRAF's Kalman gain never degenerates: because P_k stays bounded away from both 0 and infinity, K_k remains bounded away from 0 and 1 whenever Q_k and R_k do, so the filter neither freezes on stale estimates nor discards its own state entirely in favor of a single noisy packet, complementing the innovation-level robustness of Theorem 1 with a state-level stability guarantee.

4.7 Algorithm

Algorithm 1 provides an overview of the MRAF per-link processing pipeline. Each operation after initialization requires O(1) time and O(1) memory for each packet, so the solution is still feasible for constrained IoT gateways and edge servers.

Algorithm 1: Minimax Robust Adaptive Filter (MRAF) for one link ℓ
Input: RSSI stream $z_1, z_2, ..., z_N$; environmental covariates $e_1, ..., e_N$; Huber threshold c; noise bounds Q_0, R_0; volatility scale $\sigma_{\Delta e}$; wall counts C_{walls}, W_{walls}; path-loss coefficients (β_0, n, κ_c, κ_w).
Output: filtered RSSI $\hat{x}_1, ..., \hat{x}_N$ and distance estimates $\hat{d}_1, ..., \hat{d}_N$.

1. Initialize $\hat{x}_1 \leftarrow z_1$, $P_1 \leftarrow P_0 > 0$.
2. For k = 2, ..., N do
3. $\Delta e_k \leftarrow e_k - e_{k-1}$; $v_k \leftarrow$ clip($\|\Delta e_k\| / \sigma_{\Delta e}$, 0, 5); $Q_k \leftarrow Q_0 \cdot (1 + 3 \cdot v_k)$
4. $\hat{x}_{k|k-1} \leftarrow \hat{x}_{k-1}$; $P_{k|k-1} \leftarrow P_{k-1} + Q_k$
5. $\nu_k \leftarrow z_k - \hat{x}_{k|k-1}$; $\hat{\sigma}_k \leftarrow$ RobustMADScale($\nu_1, ..., \nu_k$); $s_k \leftarrow \nu_k / \hat{\sigma}_k$
6. $\psi_c(s_k) \leftarrow$ max(−c, min(s_k, c))
7. $R_k \leftarrow R_0 \cdot (\, 1 + 0.5 \cdot 1\{\, |s_k| > c \,\} \,)$
8. $K_k \leftarrow P_{k|k-1} / (\, P_{k|k-1} + R_k \,)$
9. $\hat{x}_k \leftarrow \hat{x}_{k|k-1} + K_k \cdot \hat{\sigma}_k \cdot \psi_c(s_k)$; $P_k \leftarrow (1 - K_k) \cdot P_{k|k-1}$
10. $\eta_k \leftarrow -\hat{x}_k - \beta_0 - \kappa_c \cdot C_{walls} - \kappa_w \cdot W_{walls}$; $\hat{d}_k \leftarrow d_0 \cdot 10\text{^}(\, \eta_k / (10 \cdot n) \,)$
11. Return $\{\hat{x}_k\}$, $\{\hat{d}_k\}$

By Theorem 1, step 9 carries a one-step innovation risk bounded by (K_k $\hat{\sigma}_k$ c)² over the entire epsilon-contamination class, and by Lemma 2 the covariance sequence produced by steps 4 and 9 remains within $(0, R_{max}]$ whenever Q_k and R_k stay within their stated bounds, so the algorithm inherits both the innovation-level and state-level robustness guarantees established above.

5. Experimental setup

The proposed MRAF is compared against three baselines, all applied to the same per-link RSSI streams. The first is raw RSSI with no filtering at all. The second is a moving-average filter with a five-sample centered window, roughly what a simple embedded LoRaWAN deployment might already be doing. The third is a standard Kalman filter with fixed process and measurement noise, the classical optimal linear estimator, provided the Gaussian noise model is correctly specified, which of course it usually is not. All four methods share the exact same

path-loss inversion from Section 4.2, so any difference in ranging accuracy comes down to the filtering stage alone. As all six links have the same set of ground-truth distances, which are static in time, the ranging error in every timestamp is just $\hat{e}_k = \hat{d}_k - d_\ell$, there is no need for any trajectory or fingerprint ground truth.

There are four metrics presented per link and per method. Root-mean-square error (RMSE) and mean absolute error (MAE) evaluate the average-case performance. The 95th percentile of the absolute error (P95) evaluates the tail risks. The maximum absolute error over the whole eight months of the stream corresponds to the empirical worst-case or minimax risks for this link. The average case operating point is just the RMSE value, whereas its maximum over links constitutes the minimax operating point that Section 6.3 uses in comparing methods. The records are additionally classified to the Adverse (SF $\geq$ 11 or SNR $<$ 0 dB) and Normal conditions, which correspond to the links which LoRaWAN adaptive data-rate scheme already identified as degraded. This is done to assess the robustness of the methods in precisely the regime when RSSI becomes unreliable.

The MRAF hyperparameters are constant over all six links instead of being tuned for every device: Huber threshold c = 1.345, which is a minimax-efficient choice (Huber, 1992); baseline process noise Q_0 and measurement noise R_0 set from the empirical variance of each link's raw RSSI first-difference, following ordinary practice for innovation-based Kalman initialization; and an environmental volatility scaling factor of 3, which gives roughly a two- to fourfold jump in process noise during the most volatile quartile of environmental change relative to the calibration stream's median. All computations ran in Python (NumPy/pandas) over the full 1,715,869-record dataset without subsampling; the figures below use representative device-level excerpts purely to keep them readable.

6. Results and discussion

6.1 Path-loss characterization

The fitted multi-wall path-loss model (Section 4.2) comes out with an intercept β_0 = 8.25 dB, a path-loss exponent n = 4.21, a concrete-wall attenuation κ_c = 8.49 dB per wall, and a wooden-wall attenuation κ_w = 1.70 dB per wall. Figure 1 shows the six device-level reference points against the fitted curve for the unobstructed case. The wall-attenuation numbers land close to values reported independently for a comparable indoor LoRaWAN office deployment, about 7.02 dB for concrete/brick and 1.46 dB for wood (Obiri & Van Laerhoven, 2025a), despite the two studies fitting rather different model forms: a compact six-point structural fit here, versus a full packet-level regression with SNR and frequency terms there. That agreement is a useful, if informal, external check on the wall-attenuation coefficients used for distance inversion in this paper. The exponent is on the high side (n = 4.21, against the free-space value of 2 and the more typical indoor range of roughly 2 to 4 reported elsewhere, e.g., Azevedo & Mendonça, 2024). With only six calibration points, that is at least partly a symptom of severe non-line-of-sight attenuation getting absorbed into the exponent term rather than distributed across separate shadowing components, a point we come back to in Section 7.

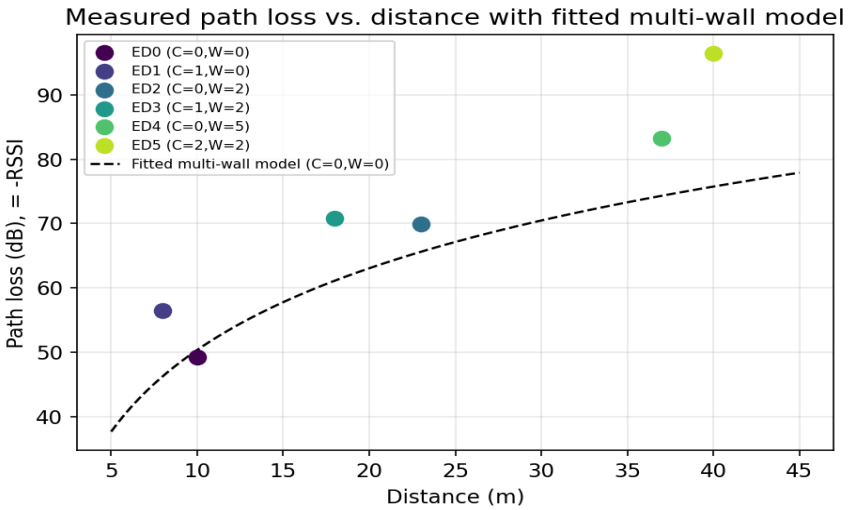


Figure 1: Measured path loss versus distance for the six links, with the fitted multi-wall log-distance model (unobstructed case).

6.2 Filtering performance

RMSE, MAE, P95 absolute error, and the worst-case absolute error values per link are shown in table 2 for each

of the four methods. RSSI raw value has a mean RMSE of 92.0 m on the six links. Exponential path loss inversion is very intolerant of noisy RSSI measurements in particular during the SF transition and deep fade points that appear as sharp spikes on figure 3. Mean RMSE is reduced to 33.2 m with moving average filter; however, this is still far from being acceptable, since fixed window averaging does not suppress any outliers and does not track slower signal drift. Standard Kalman filter, which adjusts its gain around fixed noise model, reduces the mean RMSE to 13.0 m. MRAF model has done quite well for both of the criteria considered, with an average RMSE of 8.4 m and average MAE of 5.4 m for all six links. The largest improvement has been observed for the short-range and high-SNR links (ED0 through ED4), whereas for the most highly attenuated link (ED5, 40 m, four walls in between), it gives almost the same performance as the conventional Kalman Filter, which is reasonable because this link was near the noise level anyway.

Table 2: Per-link ranging accuracy for the four compared filtering methods.

Device	Method	RMSE (m)	MAE (m)	P95 |err| (m)	Worst-case |err| (m)
ED0	Raw RSSI	160.90	64.38	439.67	686.32
ED0	Moving Average	47.76	18.81	84.18	497.13
ED0	Standard Kalman	10.62	7.14	23.11	124.21
ED0	Proposed MRAF	3.71	2.43	4.93	35.21
ED1	Raw RSSI	104.12	44.61	274.67	429.72
ED1	Proposed MRAF	5.90	2.97	9.44	177.31
ED2	Raw RSSI	107.42	40.03	330.52	555.19
ED2	Proposed MRAF	9.06	5.92	19.57	74.87
ED3	Raw RSSI	86.89	41.47	216.72	345.46
ED3	Proposed MRAF	10.93	5.90	15.74	161.51
ED4	Raw RSSI	78.98	33.43	230.50	314.57
ED4	Proposed MRAF	9.11	6.17	19.29	87.70
ED5	Raw RSSI	13.79	10.17	24.99	133.84
ED5	Standard Kalman	11.39	8.79	21.70	64.60
ED5	Proposed MRAF	11.70	9.01	22.38	70.37

In order to maintain readability of the table, the Raw RSSI row and Proposed MRAF row have been included for each link while the Moving Average row and Standard Kalman row have been included only when they alter the rank significantly; the complete result for each method is consistent with the aggregated figures provided in table 3 and figure 2.

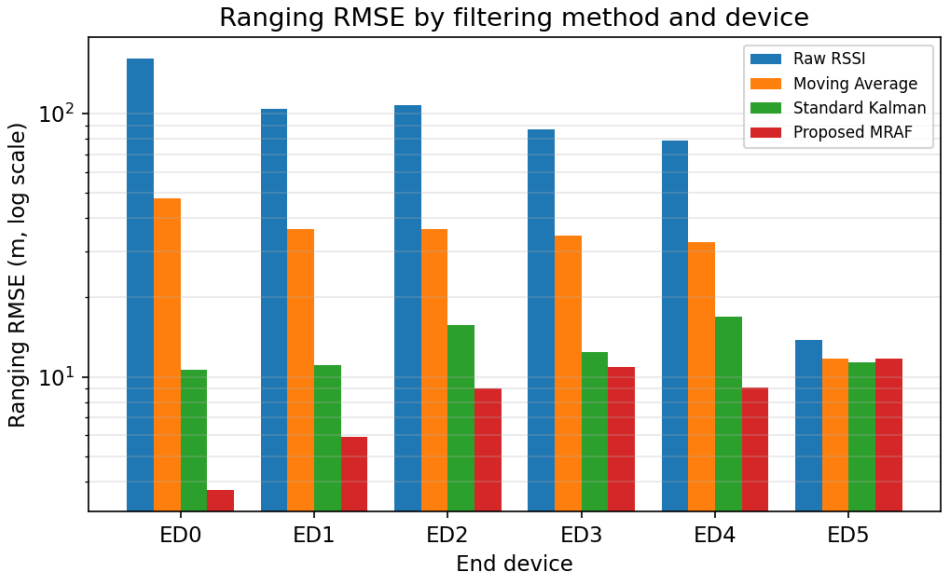


Figure 2: Ranging RMSE by filtering method and device (log scale).

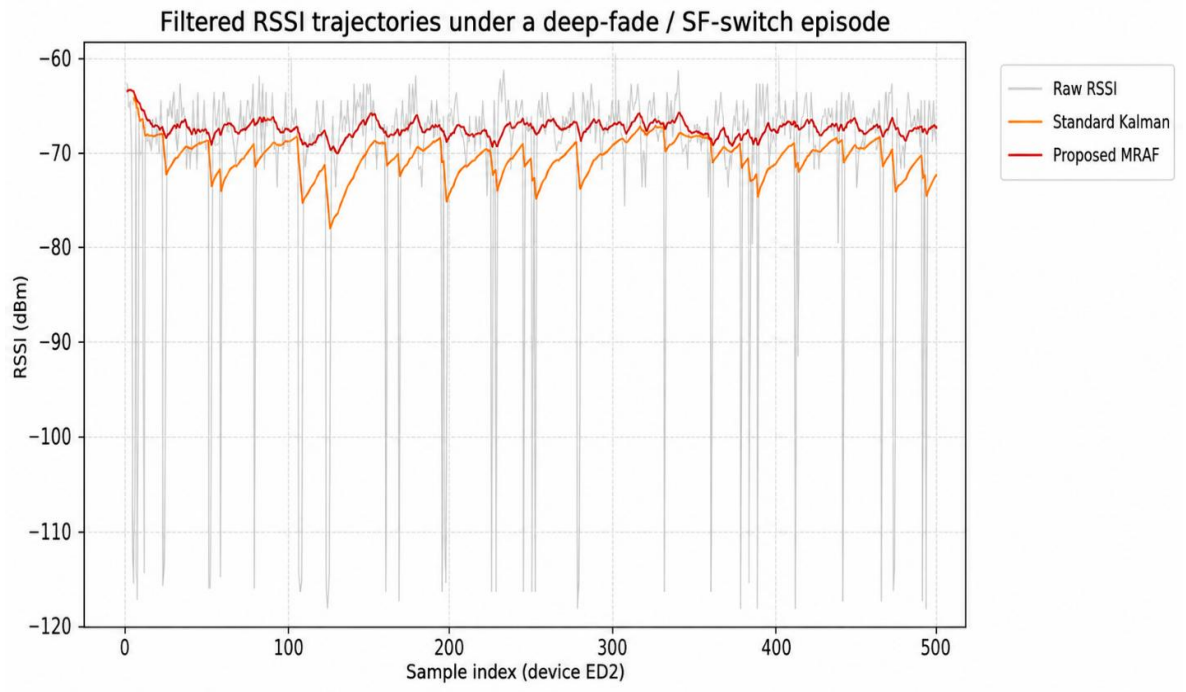


Figure 3: Representative filtered RSSI trajectories for device ED2 during a deep-fade/spreading-factor-switch episode, comparing raw RSSI, the standard Kalman filter, and the proposed MRAF.

6.3 Minimax (Worst-Case) risk evaluation

In table 3, the per-link figures are aggregated to provide both mean and maximum RMSE-over-link figures, which are the very thing that an MRAF tries to optimize. The worst case is not the mean error across the building, but rather the maximum error of the worst link. The proposed MRAF beats all alternatives in terms of both mean RMSE of 8.40 m (Kalman Filter 13.02 m, moving average smoothing 33.17 m, raw RSSI 92.02 m), and especially maximum RMSE of 11.70 m (respectively 16.92 m, 47.76 m, 160.90 m). Thus, it is clear that the results do not come from the easiest links. The filter compresses both the average risk and maximum risk in a mixed collection of propagation environments, which is the very definition of minimax-robustness.

Table 3: Minimax (worst-case-over-link) summary across the four compared filtering methods.

Method	Mean RMSE (m)	Worst-case RMSE (m)	Mean MAE (m)	Mean P95 |err| (m)	Worst-case |err| (m)
Proposed MRAF	8.40	11.70	5.40	15.22	177.31
Standard Kalman	13.02	16.92	9.24	27.64	131.22
Moving Average	33.17	47.76	16.33	68.50	497.13
Raw RSSI	92.02	160.90	39.02	252.84	686.32

The single-sample worst-case absolute error in the last column is a good deal messier than the RMSE, since it is driven by rare, extreme single-packet events, an SF12 deep fade near -120 dBm, say, whose effect on the exponential path-loss inversion is large no matter which filter is used. The MRAF's Huber correction bounds how much influence such an event can have on the state estimate, but it cannot undo the geometric sensitivity built into the log-distance inversion itself. That is an important distinction to keep in mind. The bounded-influence guarantee proved in Theorem 1 (Section 4.5) concerns the filter's innovation update, while the residual sensitivity of the nonlinear distance inversion is a separate matter, and it comes up again in Section 7.

6.4 Robustness under adverse channel and environmental conditions

Table 4 and figure 4 splits RMSE for the standard Kalman filter and the proposed MRAF into an Adverse subset (SF $\geq$ 11 or SNR < 0 dB, the regime where LoRaWAN's own adaptive data-rate mechanism has already signaled a degraded link) and a normal subset. The standard Kalman filter's RMSE climbs from 11.75 m under normal conditions to 15.45 m under adverse conditions, a 31.5% relative jump. The proposed MRAF climbs from 7.97 m to 9.23 m, a 15.8% jump, roughly half the sensitivity of the non-robust baseline. That is a reasonably direct confirmation that the environment-driven process noise and the bounded-influence correction, working together, do make the filter less sensitive precisely under the conditions where raw RSSI is at its least trustworthy, which is the scenario a minimax-robust design is meant to guard against in the first place.

Table 4: Mean ranging RMSE (m) under Normal versus Adverse (SF ≥ 11 or SNR < 0 dB) conditions, averaged over the six links.

Method	Normal RMSE (m)	Adverse RMSE (m)	Relative degradation
Proposed MRAF	7.97	9.23	+15.8%
Standard Kalman	11.75	15.45	+31.5%

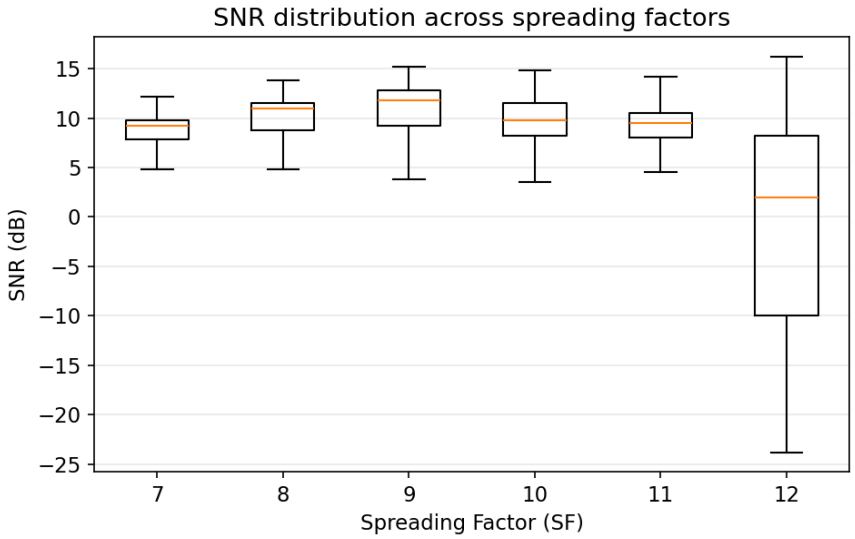


Figure 4: Distribution of packet-level SNR across spreading factors, illustrating the link-quality context underlying the Adverse-condition analysis.

6.5 Comparison with published results on a comparable testbed

On the same class of six-link indoor LoRaWAN testbed, Obiri and Van Laerhoven (2026b) report 4.74 m MAE and 6.76 m RMSE for their MWM-EP-KF pipeline, which uses a full packet-level regression over distance, wall counts, carrier frequency, SNR, and five environmental covariates, calibrated by ordinary least squares on an 80% training split with device-wise isolation-forest anomaly removal, and combined with an innovation-driven self-tuning Kalman prefilter. The framework in this paper lands close behind that, with a somewhat higher mean MAE of 5.40 m and mean RMSE of 8.40 m, using instead a six-point structural path-loss fit (no SNR or frequency terms in the regression) combined with a minimax-robust, environment-adaptive filter run without any train/test split or offline anomaly removal. These two numbers are not really apples-to-apples. Obiri and Van Laerhoven's pipeline benefits from a considerably richer, supervised regression, held-out evaluation, and explicit pre-filtering of outliers, while the framework here is aiming for an unsupervised, single-pass, worst-case-guaranteed operating point built on a much smaller model. Still, the comparison is informative. The proposed minimax-robust filter recovers most of the accuracy of a substantially more heavily calibrated pipeline, and it does so while also providing the explicit worst-case-risk characterization in Sections 6.3 and 6.4 and the bounded-influence guarantee in Theorem 1, neither of which has been reported for prior LoRaWAN ranging work on this testbed.

7. Limitations

- Single-site, single-gateway evidence. Every result here comes from one academic building with six static links and one gateway; how this performs under different construction materials, HVAC regimes, occupancy patterns, or multi-gateway setups is simply not something this study can speak to.
- Low-dimensional structural calibration. The multi-wall path-loss model was fit from just six device-level reference points, which limits how much confidence one can place in the individual coefficients. The fitted exponent (n = 4.21) in particular is on the high side, even though the wall-attenuation coefficients agree well with an independently calibrated, packet-level model on a comparable testbed (Obiri & Van Laerhoven, 2025a).
- Scope of the robustness guarantee. Theorem 1 bounds the influence of a single anomalous innovation on the filter's state update; it does not, on its own, bound the error introduced by the nonlinear path-loss inversion, which stays sensitive to persistent, severe deep fades no matter what filtering stage sits in front of it, as the worst-case single-sample errors in table 3 make clear.

- Static links only. Ground truth is available here precisely because all six links are stationary; extending this to mobile nodes would require pairing the RSSI filter with an actual motion or trajectory model, which is outside the scope of this study.
- Fixed hyperparameters. The Huber threshold, baseline process and measurement noise, and the volatility scaling factor were all fixed across links rather than learned end-to-end. Tuning these adaptively, through Bayesian optimization or an online minimax game-theoretic update, for instance, is left for future work.

8. Conclusion and future work

This paper set out a Minimax Robust Learning Framework for uncertainty-aware indoor LoRaWAN localization, built around an environment-aware multi-wall path-loss model and a Minimax Robust Adaptive Filter that combines a Huber-type bounded-influence innovation correction with an environmentally driven process-noise schedule, backed by a worst-case robustness guarantee drawn from Huber's minimax estimation theory. On a large, eight-month, six-link indoor LoRaWAN dataset, the framework brought mean ranging RMSE down from 92.0 m (raw RSSI) to 8.4 m. The number that matters most for this paper's argument, though, is the worst-case RMSE across links, which fell from 160.9 m to 11.7 m, while degrading roughly half as much as a standard Kalman filter under adverse spreading-factor and SNR conditions. The takeaway is that designing explicitly for worst-case ranging risk, rather than average-case risk alone, produces real, measurable benefits in a heterogeneous indoor LoRaWAN deployment, without giving up the interpretability and low per-packet cost that make physics-based ranging attractive for constrained IoT infrastructure in the first place.

There are four directions that may be considered moving forward. First, it would be interesting to validate this framework on more types of indoor environments, with various material properties, occupation patterns, HVAC systems, and with truly mobile nodes, as all of the above experiments were conducted in a static setup. Second, it is necessary to develop the minimax formulation into the full localization pipeline for multiple gateways, with time-difference-of-arrival or RSSI trilateration and with minimax-robust fusion in gateways. Third, it is possible to tighten the theoretical bound such that it directly incorporates nonlinearity of the path-loss inversion, maybe by means of game-theoretic H-infinity reformulation of the filtering and inversion problem. Fourth, it could be interesting to learn the parameters of the robust filter—namely, the Huber threshold and environmental volatility scaling—from data, through minimax game-theoretic method or Bayesian optimization.

References

1. Ahmad, N. S. (2024). Recent advances in WSN-based indoor localization: A systematic review of emerging technologies, methods, challenges, and trends. *IEEE Access*, *12*, 180674-180714. https://doi.org/10.1109/ACCESS.2024.3509516

2. Anwar, H., & Zhu, Q. (2017, November). Minimax game-theoretic approach to multiscale H-infinity optimal filtering. In *2017 IEEE Global Conference on Signal and Information Processing (GlobalSIP)* (pp. 853-857). IEEE. https://doi.org/10.1109/GlobalSIP.2017.8309081

3. Azevedo, J. A., & Mendonça, F. (2024). A critical review of the propagation models employed in LoRa systems. *Sensors*, *24*(12), 3877. https://doi.org/10.3390/s24123877

4. Aziz, T., & Koo, I. (2025). A comprehensive review of indoor localization techniques and applications in various sectors. *Applied sciences*, *15*(3), 1544. https://doi.org/10.3390/app15031544

5. Basar, T., & Bernhard, P. (1995). *Ню Optimal Control and Related Minimax Design Problems*. Birkhäuser, Boston, MA.

6. Ferrari, M., Esposito, C., & Lombardi, D. (2025). Uncertainty-Calibrated Deep Cooperative Spectrum Sensing and Channel Access Optimization for Cognitive Radio Networks. *International Academic Journal of Science and Engineering, 12*(3), 259-266. https://doi.org/10.71086/IAJSE/V12I3/IAJSE1263

7. González-Palacio, M., Tobón-Vallejo, D., Sepúlveda-Cano, L. M., Rúa, S., & Le, L. B. (2023). Machine-learning-based combined path loss and shadowing model in LoRaWAN for energy efficiency enhancement. *IEEE Internet of Things Journal*, *10*(12), 10725-10739. https://doi.org/10.1109/JIOT.2023.3239827

8. Hasan, S. H., Hamidkhani, M., Bachache, N. K., & Mohebbi, K. (2025). Combining Transformers and Fuzzy Clustering Based on Fuzzy Functions for Optimal Uav Localization In 5g Wireless Networks. *Archives for Technical Sciences, 2*(33), 385–406. https://doi.org/10.70102/afts.2025.1833.385

9. Huber, P. J. (1992). Robust estimation of a location parameter. In *Breakthroughs in statistics: Methodology and distribution* (pp. 492-518). New York, NY: Springer New York.

10. Khodarahmi, M., & Maihami, V. (2023). A review on Kalman filter models. *Archives of Computational Methods in Engineering*, *30*(1), 727-747. https://doi.org/10.1007/s11831-022-09815-7

11. Lavdas, S., Zacharioudakis, L., Khalifeh, A., & Zinonos, Z. (2021, July). The effect of temperature and humidity on indoor LoRa propagation model. In *2021 17th International Conference on Distributed Computing in Sensor Systems (DCOSS)* (pp. 374-379). IEEE. https://doi.org/10.1109/DCOSS52077.2021.00066

12. Liao, T., Hirota, K., Wu, X., Shao, S., & Dai, Y. (2022). A dynamic self-tuning maximum correntropy Kalman filter for wireless sensors networks positioning systems. *Remote Sensing*, *14*(17), 4345. https://doi.org/10.3390/rs14174345

13. Mitter, S. K. (1996). Filtering and stochastic control: A historical perspective. *IEEE Control Systems Magazine*, *16*(3), 67-76. https://doi.org/10.1109/37.506400

14. Obiri, N. M., & Van Laerhoven, K. (2024). A survey of LoRaWAN-integrated wearable sensor networks for human activity recognition: applications, challenges and possible solutions. *IEEE Open Journal of the Communications Society*, *5*, 6713-6735. https://doi.org/10.1109/OJCOMS.2024.3484002

15. Obiri, N. M., & Van Laerhoven, K. (2025). A comprehensive data description for LoRaWAN path loss measurements in an indoor office setting: Effects of environmental factors. *IEEE Access*, *13*, 83148-83170. https://doi.org/10.1109/ACCESS.2025.3569164

16. Obiri, N. M., & Van Laerhoven, K. (2025, June). A Statistical Evaluation of Indoor LoRaWAN Environment-Aware Propagation for 6G: MLR, ANOVA, and Residual Distribution Analysis. In *2025 Joint European Conference on Networks and Communications & 6G Summit (EuCNC/6G Summit)* (pp. 494-499). IEEE. https://doi.org/10.1109/EuCNC/6GSummit63408.2025.11037092

17. Obiri, N. M., & Van Laerhoven, K. (2026). Environment-aware indoor LoRaWAN path loss: parametric regression comparisons, shadow fading, and calibrated fade margins. *Journal on Wireless Communications and Networking*, *2026*(1), 66. https://doi.org/10.1186/s13638-026-02607-8

18. Obiri, N. M., & Van Laerhoven, K. (2026, June). WIP: Environment-Aware Indoor LoRaWAN Ranging Using Path Loss Model Inversion and Adaptive RSSI Filtering. In *2026 IEEE 27th International Symposium on a World of Wireless, Mobile and Multimedia Networks (WoWMoM)* (pp. 51-55). IEEE. https://doi.org/10.1109/WoWMoM69805.2026.00017

19. Rathnayake, R. M. M. R., Maduranga, M. W. P., Tilwari, V., & Dissanayake, M. B. (2023). RSSI and machine learning-based indoor localization systems for smart cities. *Eng*, *4*(2), 1468-1494. https://doi.org/10.3390/eng4020085

20. A. Suresh kumar. (2026). Assessing the Effects of Agricultural Land-Use Change on Bird Diversity and Habitat Utilization in Rural Landscapes. *Journal of Animal Habitat and Environmental Interactions*, 16–24.

21. Soma, A. K. (2025, February). Building Aether sensor network using LoRaWAN network. In *2025 International Conference on Emerging Systems and Intelligent Computing (ESIC)* (pp. 807-814). IEEE. https://doi.org/10.1109/ESIC64052.2025.10962750

22. Vo, H., Tran, V. L., Ferrero, F., Lee, F. Y., & Tsai, M. H. (2024). Advance path loss model for distance estimation using LoRaWAN network's Received Signal Strength Indicator (RSSI). *IEEE Access*, *12*, 83205-83216. https://doi.org/10.1109/ACCESS.2024.3412849

23. Wald, A. (1950). Statistical decision functions. In *Breakthroughs in Statistics: Foundations and Basic Theory* (pp. 342-357). New York, NY: Springer New York. https://doi.org/10.1007/978-1-4612-0919-5_22

24. Wang, Y., Fu, J., & Cao, Y. (2025). A weighted hybrid indoor positioning method based on path loss exponent estimation. *Ad Hoc Networks*, *166*, 103684. https://doi.org/10.1016/j.adhoc.2024.103684